

Fast Pairwise Conversion of Supernova Neutrinos: A Dispersion Relation Approach

Ignacio Izaguirre,¹ Georg Raffelt,¹ and Irene Tamborra²

¹Max-Planck-Institut für Physik (Werner-Heisenberg-Institut), Föhringer Ring 6, 80805 München, Germany

²Niels Bohr International Academy, Niels Bohr Institute, Blegdamsvej 17, 2100 Copenhagen, Denmark

(Received 10 October 2016; published 10 January 2017)

Collective pair conversion $\nu_e \bar{\nu}_e \leftrightarrow \nu_x \bar{\nu}_x$ by forward scattering, where $x = \mu$ or τ , may be generic for supernova neutrino transport. Depending on the local angular intensity of the electron lepton number carried by neutrinos, the conversion rate can be “fast,” i.e., of the order of $\sqrt{2}G_F(n_{\nu_e} - n_{\bar{\nu}_e}) \gg \Delta m_{\text{atm}}^2/2E$. We present a novel approach to understand these phenomena: a dispersion relation for the frequency and wave number (Ω, \mathbf{K}) of disturbances in the mean field of $\nu_e \nu_x$ flavor coherence. Runaway solutions occur in “dispersion gaps,” i.e., in “forbidden” intervals of Ω and/or \mathbf{K} where propagating plane waves do not exist. We stress that the actual solutions also depend on the initial and/or boundary conditions, which need to be further investigated.

DOI: 10.1103/PhysRevLett.118.021101

Introduction.—The physics of core-collapse supernova (SN) explosions and neutron-star (NS) mergers raise unique questions about flavor evolution in environments where neutrinos are dense. Their decoupling strongly depends on flavor because β reactions dominate for ν_e and $\bar{\nu}_e$. As a result, the $\nu_e \bar{\nu}_e$ flux of the SN accretion phase exceeds the $\nu_x \bar{\nu}_x$ fluxes [1], an effect that is even more pronounced in NS mergers [2,3]. Moreover, the SN ν_e flux is larger than the $\bar{\nu}_e$ one (deleptonization) and the other way around in NS mergers.

The subsequent flavor evolution matters because SN neutrinos not only carry away energy, but also deposit some of it in the gain region below the stalled SN shock by $\nu_e + n \rightarrow p + e^-$ and $\bar{\nu}_e + p \rightarrow n + e^+$, thus driving the delayed explosion. At later stages, neutrinos regulate the nucleosynthesis outcome in the neutrino-driven wind. The neutrino signal from the next nearby SN will also depend on the flavor ratio.

In the SN region of interest, the matter density is large and suppresses conventional flavor conversion of the type $\nu_e(\mathbf{p}) \rightarrow \nu_x(\mathbf{p})$, which is driven by neutrino masses and mixing. This effect becomes important only at larger radii where neutrinos undergo an MSW resonance [4]. Stochastic density variations from turbulence might stimulate flavor conversions [5], but have been found to be ineffective during the accretion phase [6].

Neutrino-neutrino interactions can famously change this picture [1,7–15] because flavor off-diagonal refraction by $\nu_e \nu_x$ coherence spawns conversion [16–18]. In this way, neutrinos feed back upon themselves and can develop collective runaway modes. Neutral-current interactions preserve flavor, so we are dealing with flavor exchange of the type $\nu_e(\mathbf{p}) + \nu_x(\mathbf{k}) \leftrightarrow \nu_x(\mathbf{p}) + \nu_e(\mathbf{k})$ and especially $\nu_e(\mathbf{p}) + \bar{\nu}_e(\mathbf{k}) \leftrightarrow \nu_x(\mathbf{p}) + \bar{\nu}_x(\mathbf{k})$ by forward scattering. Such pairwise swaps preserve net flavor, but still modify subsequent charged-current interactions.

The impact of refractive $\nu_e \bar{\nu}_e \leftrightarrow \nu_x \bar{\nu}_x$ conversion has never been studied in SN simulations because such effects

seemed to arise only beyond the shock wave [19]. Yet, Sawyer has long held that such conclusions result from overly simplified assumptions about neutrino distributions [20–22] and recently, other authors have followed suit [23,24]. The key issue is the ν_e and $\bar{\nu}_e$ angle distributions to be sufficiently different, in contrast to the traditional “bulb” emission model. Another option is a “backward” ν_e and $\bar{\nu}_e$ flux, which is unavoidable in the SN decoupling region and also at larger distances [25,26]. The growth rate for “fast multiangle instabilities” is of the order of

$$\Phi_0 = \sqrt{2}G_F(n_{\nu_e} - n_{\bar{\nu}_e}) = 6.42 \text{ m}^{-1} \frac{n_{\nu_e} - n_{\bar{\nu}_e}}{10^{31} \text{ cm}^{-3}}. \quad (1)$$

Notice that we use natural units with $\hbar = c = 1$, where $6.42 \text{ m}^{-1} = 1.92 \times 10^9 \text{ s}^{-1} = 1.27 \mu\text{eV}$. This rate is “fast” in that it far exceeds the vacuum oscillation frequency $\Delta m_{\text{atm}}^2/2E = 0.5 \text{ km}^{-1}$ where we have used $\Delta m_{\text{atm}}^2 = 2.4 \times 10^{-3} \text{ eV}^2$ and $E = 12.5 \text{ MeV}$. Fast flavor conversion does not require neutrino masses or mixing, except for providing seed perturbations. Moreover, energy drops out, forestalling the characteristic energy-dependent flavor swaps found in many scenarios of collective flavor conversion [1,9]. More likely, some sort of flavor equilibration by chaotic evolution of many nonlinearly coupled modes will occur [20–22,27–30].

We here propose a new perspective that vastly simplifies both the conceptual understanding and the practical treatment of these phenomena. The starting point is the mean field of $\nu_e \nu_x$ coherence, essentially the off-diagonal element of the usual $\varrho(t, \mathbf{r}, \mathbf{p})$ flavor matrix, which normally evolves purely kinematically. However, after including $\nu\nu$ refraction, ϱ becomes dynamical and we can think of the neutrino medium as supporting flavor waves described by a wave four vector $K = (\Omega, \mathbf{K})$ and a corresponding polarization vector.

A propagating mode is a collective disturbance with a certain frequency Ω . To fulfill the equation of motion

(EOM), Ω may be required to be complex for some \mathbf{K} , leading to solutions which grow or shrink exponentially in time. Conversely, some Ω specified at the boundary may require complex \mathbf{K} and thus, exponential solutions as a function of distance. Moreover, various recently discovered symmetry-breaking effects [31–36] simply correspond to complex \mathbf{K} in directions other than the symmetry axis of the neutrino medium and/or to different polarizations of our flavor waves. We here focus on fast modes because they are less familiar, yet may dominate in environments where previously no conversion was thought to occur.

Mean field of flavor coherence.—We describe the neutrino mean field by the usual density matrices ρ . For two flavors, we write in the weak-interaction basis

$$\rho = \frac{f_{\nu_e} + f_{\nu_x}}{2} + \frac{f_{\nu_e} - f_{\nu_x}}{2} \begin{pmatrix} s & S \\ S^* & -s \end{pmatrix}, \quad (2)$$

where f_{ν_e} and f_{ν_x} are the initial occupation numbers. The complex scalar field $S_{\mathbf{p}}(t, \mathbf{r})$ represents $\nu_e \nu_x$ flavor coherence for mode \mathbf{p} , whereas the real field $s_{\mathbf{p}}(t, \mathbf{r})$ obeys $s_{\mathbf{p}}^2 + |S_{\mathbf{p}}|^2 = 1$ and provides the survival probability by $\frac{1}{2}(1 + s)$. We use the “flavor isospin convention,” where $\bar{\nu}$ has negative energy and negative ρ , so the $\bar{\nu}$ coefficients are $-(f_{\bar{\nu}_e} + f_{\bar{\nu}_x})/2$ and $-(f_{\bar{\nu}_e} - f_{\bar{\nu}_x})/2$.

The usual EOM is $(\partial_t + \mathbf{v} \cdot \nabla_{\mathbf{r}})\rho = i[\rho, \mathbf{H}]$, where we ignore collisions [37,38] and where the Liouville operator accounts for free streaming. The Hamiltonian matrix is $\mathbf{H} = \mathbf{M}^2/2E + v^\mu \Lambda_\mu \frac{1}{2} \sigma_3 + \sqrt{2} G_F \int d\Gamma' v^\mu v'_\mu Q'$, where σ_3 is a Pauli matrix. The neutrino mass-square matrix \mathbf{M}^2 is what drives oscillations because it is not diagonal in the weak interaction basis. The second term is the usual matter effect, where $v^\mu \Lambda_\mu = \Lambda_0 - \mathbf{v} \cdot \Lambda$, $v^\mu = (1, \mathbf{v})$ is the neutrino four velocity, and $\Lambda_0 = \sqrt{2} G_F (n_e - n_{\bar{e}})$, with Λ the corresponding current. The third term is an integral over the neutrino phase space, extending to negative energies to include antineutrinos.

We here study fast modes and thus, dismiss \mathbf{M}^2 . As neutrinos are produced in flavor states, any ρ matrix beginning and staying diagonal is a fixed-point solution. Our task is to determine when this fixed point is stable or unstable. To this end, we use $|S| \ll 1$ and observe that to linear order $s = \sqrt{1 - |S|^2} = 1$. Moreover, the EOM no longer depends on E , so we only deal with angle modes described by \mathbf{v} . The same $S_{\mathbf{v}}$ applies to ν and $\bar{\nu}$, so we only need the angle distribution of electron lepton number (ELN) carried by neutrinos, which we express as

$$G_{\mathbf{v}} = \sqrt{2} G_F \int_0^\infty \frac{dE E^2}{2\pi^2} [f_{\nu_e}(E, \mathbf{v}) - f_{\bar{\nu}_e}(E, \mathbf{v})]. \quad (3)$$

If the ν_x and $\bar{\nu}_x$ distributions are not equal, we must include $-[f_{\nu_x}(E, \mathbf{v}) - f_{\bar{\nu}_x}(E, \mathbf{v})]$. The ELN potential is $\Phi_0 = \int d\Gamma G_{\mathbf{v}}$, and the current is $\Phi = \int d\Gamma G_{\mathbf{v}} \mathbf{v}$. The phase-space

integration is over the unit sphere: $\int d\Gamma = \int d\mathbf{v}/4\pi$. We may use coordinates with z along the radial direction and angles (θ, φ) to express $\mathbf{v} = (v_x, v_y, v_z) = (s_\theta c_\varphi, s_\theta s_\varphi, c_\theta)$, where $c_\theta = \cos(\theta)$ and so on.

Assuming that in our test volume, the occupation numbers, as well as the matter density, are homogeneous and stationary, the linearized EOM is

$$i(\partial_t + \mathbf{v} \cdot \nabla_{\mathbf{r}})S_{\mathbf{v}} = v^\mu (\Lambda + \Phi)_\mu S_{\mathbf{v}} - \int d\Gamma' v^\mu v'_\mu G_{\mathbf{v}'} S_{\mathbf{v}'}. \quad (4)$$

Here, $v^\mu (\Lambda + \Phi)_\mu = \Lambda_0 + \Phi_0 - \mathbf{v} \cdot (\Lambda + \Phi)$ is the energy shift due to *matter and neutrinos* and $v^\mu v'_\mu = (1 - \mathbf{v} \cdot \mathbf{v}')$. For plane wave, $S_{\mathbf{v}}(t, \mathbf{r}) = Q_{\mathbf{v}}(\Omega, \mathbf{K}) e^{-i(\Omega t - \mathbf{K} \cdot \mathbf{r})}$, the EOM is

$$v^\mu k_\mu Q_{\mathbf{v}} = - \int d\Gamma' v^\mu v'_\mu G_{\mathbf{v}'} Q_{\mathbf{v}'}, \quad (5)$$

where $k = K - (\Lambda + \Phi)$, with $k^\mu = (\omega, \mathbf{k})$ and $K = (\Omega, \mathbf{K})$. Notice that our ω does not denote $\Delta m_{\text{atm}}^2/2E$.

The dispersion relation will be for (ω, \mathbf{k}) and depends only on $G_{\mathbf{v}}$. Matter enters through the constant shift $(\Omega, \mathbf{K}) \rightarrow (\omega, \mathbf{k})$, which means going to a rotating frame in flavor space [18,29,39]. K and k have the same imaginary part, if any. The shift amounts to a global gauge transformation $S_{\mathbf{p}}(r) \rightarrow S_{\mathbf{p}}(r) e^{i(\Lambda + \Phi)r}$. For the ρ matrices, it is a global SU(2) gauge transformation.

Dispersion relation (DR).—Without $\nu\nu$ interactions, Eq. (5) implies $v^\mu k_\mu = 0$. This purely kinematical relation means that a spatial disturbance of mode \mathbf{v} is carried by the Liouville flow, causing a local time variation with $\omega = \mathbf{v} \cdot \mathbf{k}$. Including $\nu\nu$ interactions, the EOM becomes dynamical. Physically, the local time variation “observed” by another neutrino can lead to a parametric resonance and thus, to runaway solutions.

The right hand side of Eq. (5) has the form $v^\mu a_\mu$, with a “polarization vector” $a_\mu = - \int d\Gamma' v_\mu G_{\mathbf{v}'} Q_{\mathbf{v}'}$, so $Q_{\mathbf{v}} = v^\mu a_\mu / v^\mu k_\mu$. Insertion on both sides of Eq. (5) yields $v^\mu a_\mu = - \int d\Gamma' v^\mu v'_\mu G_{\mathbf{v}'} a^\mu v'_\mu / k^\mu v'_\mu$. Using the metric $\eta^{\mu\nu} = \text{diag}(+, -, -, -)$, this EOM is $v_\mu \Pi^{\mu\nu} a_\nu = 0$. Here the “polarization tensor,”

$$\Pi^{\mu\nu} = \eta^{\mu\nu} + \int \frac{d\mathbf{v}}{4\pi} G_{\mathbf{v}} \frac{v^\mu v^\nu}{\omega - \mathbf{v} \cdot \mathbf{k}}, \quad (6)$$

contains all physical information, which derives from the ELN angle distribution $G_{\mathbf{v}}$. The EOM $v_\mu \Pi^{\mu\nu} a_\nu = 0$ applies to any mode v_μ and thus, amounts to

$$\Pi^{\mu\nu} a_\nu = 0. \quad (7)$$

The latter has nontrivial solutions for $\det[\Pi^{\mu\nu}(k)] = 0$, providing the DR. Once we have found solutions $k^\mu = (\omega, \mathbf{k})$, we can identify the corresponding polarization vector a^μ and the eigenfunction $Q_{\mathbf{v}} = a^\mu v_\mu / k^\mu v_\mu$.

To find propagating modes with real k , we first pick a direction $\hat{\mathbf{k}}$ and write $\mathbf{k} = \hat{\mathbf{k}}n\omega$ in terms of the refractive index n . In Eq. (6), we now pull $1/\omega$ out of the integral and recognize that $\det[\Pi^{\mu\nu}] = 0$ is a quartic equation for ω as a function of n ; i.e., instead of $n(\omega)$, we find four branches $\omega(n)$. Considering $\mathbf{k}(n) = \hat{\mathbf{k}}n\omega(n)$, we thus find parametric solutions in the form $[\omega(n), \mathbf{k}(n)]$. On the other hand, there is no obvious elegant way to find complex ω solutions for real \mathbf{k} or the other way around without searching for roots of $\det[\Pi^{\mu\nu}(k)] = 0$.

Generic example.—We assume axial symmetry of G_{ν} and pick \mathbf{k} in the radial direction (z). In $\Pi^{\mu\nu}$, all terms linear in $v_{x,y}$ vanish, so Eq. (7) yields two equations for (a_0, a_z) , providing $Q_{\nu} = (a_0 - a_z c_{\theta})/(\omega - k_z c_{\theta})$ where we have used $\mathbf{k} = (0, 0, k_z)$. These are the bimodal and multizimuth angle (MZA) polarizations [32], which are axially symmetric. The diagonal $\Pi^{\mu\nu}$ terms from v_x^2 and v_y^2 yield degenerate solutions for $a_{x,y}$, with $Q_{\nu} = -(a_x s_{\theta} c_{\phi} + a_y s_{\theta} s_{\phi})/(\omega - k_z c_{\theta})$, the axial symmetry-breaking multiazimuth angle (MAA) polarizations.

To be explicit, we study the simplest nontrivial case: two θ modes representing two zenith ranges, i.e., $G_{\nu} = G_1 \delta(c_{\theta} - c_1) + G_2 \delta(c_{\theta} - c_2)$. The axially symmetric polarizations produce a quadratic form in both ω and k_z , implying that the DRs are hyperbolas in the ω - k_z plane, as shown in Fig. 1. The axially breaking polarizations provide similar results.

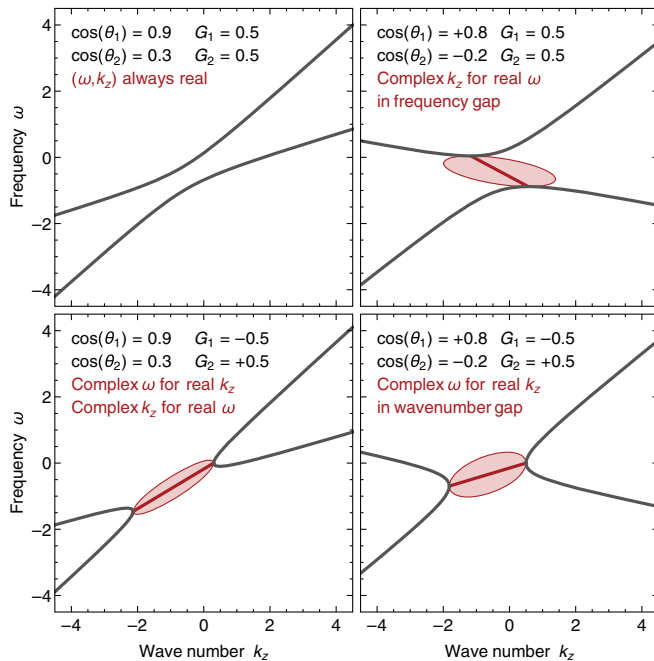


FIG. 1. Dispersion relations (black lines) for two θ modes. The thick red line is $\text{Re}(\omega)$ for real k_z or $\text{Re}(k_z)$ for real ω . The width of the blob is $\pm \text{Im}(\omega)$ or $\pm \text{Im}(k_z)$. Left: Only outward modes. Right: One outward and one backward mode. Top: Both ν_e excess. Bottom: Forward mode $\bar{\nu}_e$ excess.

The left panels use forward modes ($0 < \cos \theta_{1,2} < 1$) as in traditional bulb emission. If ν_e dominates in both modes (upper left), both ω and k_z are real: no fast flavor conversion occurs. If one mode has a $\bar{\nu}_e$ excess ($G_1 < 0$), the DR has a gap, providing complex ω for real k_z and the other way around, as indicated by the red blob. Disturbances with k_z in the gap grow exponentially in time. A real ω imposed at the boundary causes exponential spatial growth. These conclusions carry over to more general $G(\theta)$ where one needs a crossing from positive to negative ELN intensities to obtain a dispersion gap, which, in turn, enables fast flavor conversion, similar to spectral crossings for slow modes [40–42].

One forward and one backward mode with ν_e excess (upper right) produce two branches of real ω for all k_z , but an ω gap. All spatial disturbances propagate, but a “forbidden” frequency imposed at the boundary causes exponential spatial growth. If instead, one of our two modes has $\bar{\nu}_e$ excess (lower right), there is a gap in k_z . Wave numbers in this range imply temporal run away.

The direction of a general \mathbf{k} can be chosen such that it feels forward and backward modes, even if all modes are forward in the SN frame. If $G_{\nu} > 0$ everywhere (no crossing), such cases produce a DR analogous to the upper right panel (an ω gap). The neutrino flow is a very anisotropic medium, so dispersion strongly depends on $\hat{\mathbf{k}}$. Moreover, some components of \mathbf{k} may be real and only one of them complex, producing exponential variation in only one spatial direction for a certain ω gap.

Realistic distribution.—The flavor-dependent neutrino angle distributions from SN simulations are not readily available. To gain intuition, we have extracted the ELN distributions from a Garching simulation of a $15M_{\odot}$ progenitor [26,43,44]. Figure 2 shows a typical case not far from the decoupling region. For larger distances, the ELN profile is horizontally compressed near the forward ($\cos \theta = 1$) direction, although backward modes ($\cos \theta < 0$) are never empty. One key feature is the forward

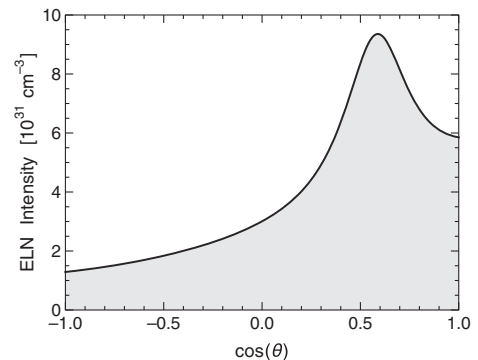


FIG. 2. Electron lepton number (ELN) angle distribution G_{θ} of a $15M_{\odot}$ SN simulation at 280 ms post bounce and a radius 37 km. We plot an ELN number density, to be converted to a weak potential by Eq. (1). We show a mildly smoothed approximation suitable for analytic post processing.

dip due to $\bar{\nu}_e$ being more forward peaked than ν_e . However, we have not found any place or time in this model where this dip would go negative.

Figure 3 shows the DR implied by G_θ of Fig. 2 for a radial-moving mode with $\mathbf{k} = (0, 0, k_z)$. Without $\nu\nu$ interactions, the DR is $\omega = c_\theta k_z$ for any angle mode c_θ (gray-shaded region). Including $\nu\nu$ interactions, this region becomes a “zone of avoidance” for propagating collective oscillations as $Q_\nu \propto 1/(\omega - c_\theta k_z)$ would be singular. The thick blue lines are the dispersion relations for the axially symmetric polarizations. The two degenerate axially breaking ones (thick orange) end at the big dots on the border of the zone of avoidance. In the frequency gap, k_z is complex. We show its real part by semithick blue and orange lines ending on the horizontal axis. In analogy to the red blobs in Fig. 1, the blue and orange shaded regions which kiss the dispersion curves indicate the imaginary part of k_z ; i.e., k_z in the frequency gap has a real part (semithick line) plus or minus an imaginary part (edge of the blob).

Growth in the gap.—Any type of ELN distribution probably occurs somewhere in NS mergers or 3D SN models, but in our 1D model, G_ν is always positive and has no crossings. Hence, dispersion is similar to an EM wave in plasma: For every \mathbf{k} there is a real ω , but there is an ω gap where the EOM requires \mathbf{k} to be complex.

In analogy to the stability analyses for slow modes [45], exponential spatial growth obtains if at an interface (e.g., the neutrino sphere), a forbidden frequency is prescribed. The latter was chosen to be stationary in the frame where M^2 is static, i.e., $\Omega = \omega + \Lambda_0 + \Phi_0 = 0$, and the system was stable (real \mathbf{K}) in this region. However, the matter

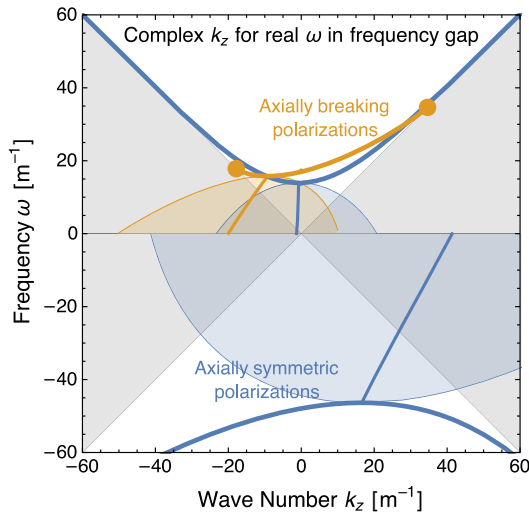


FIG. 3. Dispersion relations for $\mathbf{k} = (0, 0, k_z)$, with G_θ shown in Fig. 2. Blue: Axially symmetric polarizations. Orange: Two degenerate axially breaking polarizations. Dots: End of a branch. Filled regions: Complex solutions in analogy to the red blobs in Fig. 1, where the semithick solid line is $\text{Re}(k_z)$, and the edge of the blob indicates $\pm\text{Im}(k_z)$. Gray region: Zone of avoidance for real (ω, k_z) .

density and neutrino angle distribution evolve with radius, so a propagating wave can enter a forbidden frequency band. Exponentially damping and growing solutions ensue, the latter ones quickly taking over. Beginning with Ref. [7], such exponential growth starting at some “onset radius” has been found in many numerical studies.

Notice the difference to EM waves entering a forbidden region, e.g., radio waves in the ionized upper atmosphere. The plasma frequency prevents propagation and they are reflected—they do not grow exponentially in the ionosphere. Flavor waves obey a first-order differential equation, probably explaining this difference.

Recently, it was argued that one should not pick $\Omega = 0$ *a priori* because every frequency would have *some* amplitude at the boundary [29,39]. In this case, the system is spatially unstable everywhere if it has a frequency gap.

Boundary conditions.—However, it is not obvious that the picture of the flavor field being driven by an external frequency at some “neutrino sphere” is an appropriate description altogether. Ignoring collisions and without a *physical* interface, the EOM applies on both sides of an assumed boundary surface. The length scales for fast flavor conversion are small, so something like the traditional bulb model is not justified in any obvious sense. Furthermore, the inclusion of backward modes may require to specify boundary conditions in different spatial regions. In a SN, all inward-moving neutrinos come from neutral-current scattering of the outward moving ones; hence, inward and outward flows are flavor correlated beyond what is prescribed by the EOM.

The DR alone only indicates which solutions are consistent with the EOM, but not which ones will actually occur. We would be sure that the system was always stable if the DR did not have any gaps, which, however, seem to be generic. Except for quantum fluctuations or hypothetical flavor-violating interactions [46–48], M^2 is the only source of seed perturbations. However, which spectrum of flavor disturbances is produced, and where, remains to be better understood.

Summary.—We have derived a general dispersion relation (DR) for disturbances in the mean field of $\nu_e\nu_x$ coherence. This approach corroborates that fast runaway solutions can indeed occur as first shown by Sawyer. We have found that it is the local ν_e minus $\bar{\nu}_e$, angle distribution G_ν , that drives this effect. Therefore, G_ν should be investigated in a larger class of SN models, notably in 3D simulations exhibiting the LESA effect [49]. The presence of “crossings” in G_ν would signify \mathbf{k} gaps in the DR and concomitant *temporal* instabilities, which depend on the *initial* conditions of the flavor disturbances.

At present, it looks like ω gaps are the most generic dispersion form, so the spatial boundary conditions and their time variation are needed to understand the generic behavior of the flavor field. Eventually, one may not get around, including the collision term in the EOM, to see which modes of the flavor field are actually excited.

While the DR alone does not prove that fast pairwise flavor conversion indeed occurs, it may well be a generic phenomenon for SN neutrinos. The impact of flavor equilibration in the decoupling region should be phenomenologically explored. The relevant length scales are much smaller than the resolution of SN simulations, so one anyway needs a schematic implementation. Although the details remain speculative, nontrivial modifications of shock reheating may be expected.

G. R. acknowledges partial support by the Deutsche Forschungsgemeinschaft (Grant No. EXC 153) and the Horizon-2020 Marie Skłodowska-Curie Actions of the European Union (Grant No. H2020-MSCA-ITN-2015/674896-ELUSIVES). I. T. acknowledges support from the Knud Højgaard Foundation, the Villum Foundation (Project No. 13164) and the Danish National Research Foundation (DNRF91). We thank the Institute for Nuclear Theory at the University of Washington for hospitality and the DOE for partial support during early stages of this work.

-
- [1] A. Mirizzi, I. Tamborra, H.-T. Janka, N. Saviano, K. Scholberg, R. Bollig, L. Hüdepohl, and S. Chakraborty, Supernova neutrinos: Production, oscillations and detection, *Riv. Nuovo Cimento* **39**, 1 (2016).
- [2] F. Foucart, R. Haas, M. D. Duez, E. O'Connor, C. D. Ott, L. Roberts, L. E. Kidder, J. Lippuner, H. P. Pfeiffer, and M. A. Scheel, Low mass binary neutron star mergers: Gravitational waves and neutrino emission, *Phys. Rev. D* **93**, 044019 (2016).
- [3] A. Malkus, G. C. McLaughlin, and R. Surman, Symmetric and standard matter-neutrino resonances above merging compact objects, *Phys. Rev. D* **93**, 045021 (2016).
- [4] S. P. Mikheev and A. Yu. Smirnov, Neutrino oscillations in a variable density medium and neutrino bursts due to the gravitational collapse of stars, *Zh. Eksp. Teor. Fiz.* **91**, 7 (1986); *Sov. Phys. JETP* **64**, 4 (1986).
- [5] K. M. Patton, J. P. Kneller, and G. C. McLaughlin, Stimulated neutrino transformation through turbulence on a changing density profile and application to supernovae, *Phys. Rev. D* **91**, 025001 (2015).
- [6] J. P. Kneller, Turbulence and neutrinos during the accretion phase, in *Flavor Observations with Supernova Neutrinos*, 2016, http://www.int.washington.edu/talks/WorkShops/int_16_61W/People/Kneller_J/Kneller.pdf.
- [7] H. Duan, G. M. Fuller, J. Carlson, and Y.-Z. Qian, Simulation of coherent non-linear neutrino flavor transformation in the supernova environment: Correlated neutrino trajectories, *Phys. Rev. D* **74**, 105014 (2006).
- [8] H. Duan and J. P. Kneller, Neutrino flavour transformation in supernovae, *J. Phys. G* **36**, 113201 (2009).
- [9] H. Duan, G. M. Fuller, and Y.-Z. Qian, Collective neutrino oscillations, *Annu. Rev. Nucl. Part. Sci.* **60**, 569 (2010).
- [10] S. Chakraborty, R. Hansen, I. Izaguirre, and G. G. Raffelt, Collective neutrino flavor conversion: Recent developments, *Nucl. Phys.* **B908**, 366 (2016).
- [11] S. Hannestad, G. G. Raffelt, G. Sigl, and Y. Y. Y. Wong, Self-induced conversion in dense neutrino gases: Pendulum in flavour space, *Phys. Rev. D* **74**, 105010 (2006); Erratum, *Phys. Rev. D* **76**, 029901(E) (2007).
- [12] G. G. Raffelt and G. Sigl, Self-induced decoherence in dense neutrino gases, *Phys. Rev. D* **75**, 083002 (2007).
- [13] G. L. Fogli, E. Lisi, A. Marrone, A. Mirizzi, and I. Tamborra, Low-energy spectral features of supernova (anti) neutrinos in inverted hierarchy, *Phys. Rev. D* **78**, 097301 (2008).
- [14] Y. Pehlivan, A. B. Balantekin, T. Kajino, and T. Yoshida, Invariants of collective neutrino oscillations, *Phys. Rev. D* **84**, 065008 (2011).
- [15] C. Volpe, D. Väänänen, and C. Espinoza, Extended evolution equations for neutrino propagation in astrophysical and cosmological environments, *Phys. Rev. D* **87**, 113010 (2013).
- [16] J. T. Pantaleone, Neutrino oscillations at high densities, *Phys. Lett. B* **287**, 128 (1992).
- [17] S. Samuel, Neutrino oscillations in dense neutrino gases, *Phys. Rev. D* **48**, 1462 (1993).
- [18] H. Duan, G. M. Fuller, and Y.-Z. Qian, Collective neutrino flavor transformation in supernovae, *Phys. Rev. D* **74**, 123004 (2006).
- [19] B. Dasgupta, E. P. O'Connor, and C. D. Ott, The role of collective neutrino flavor oscillations in core-collapse supernova shock revival, *Phys. Rev. D* **85**, 065008 (2012).
- [20] R. F. Sawyer, Speed-up of neutrino transformations in a supernova environment, *Phys. Rev. D* **72**, 045003 (2005).
- [21] R. F. Sawyer, The multi-angle instability in dense neutrino systems, *Phys. Rev. D* **79**, 105003 (2009).
- [22] R. F. Sawyer, Neutrino Cloud Instabilities just above the Neutrino Sphere of a Supernova, *Phys. Rev. Lett.* **116**, 081101 (2016).
- [23] S. Chakraborty, R. S. Hansen, I. Izaguirre, and G. G. Raffelt, Self-induced neutrino flavor conversion without flavor mixing, *J. Cosmol. Astropart. Phys.* **03** (2016) 042.
- [24] B. Dasgupta, A. Mirizzi, and M. Sen, Fast neutrino flavor conversions near the supernova core with realistic flavor-dependent angular distributions, [arXiv:1609.00528](https://arxiv.org/abs/1609.00528).
- [25] J. F. Cherry, J. Carlson, A. Friedland, G. M. Fuller, and A. Vlasenko, Neutrino Scattering and Flavor Transformation in Supernovae, *Phys. Rev. Lett.* **108**, 261104 (2012).
- [26] S. Sarikas, I. Tamborra, G. G. Raffelt, L. Hüdepohl, and H.-T. Janka, Supernova neutrino halo and the suppression of self-induced flavor conversion, *Phys. Rev. D* **85**, 113007 (2012).
- [27] R. S. Hansen and S. Hannestad, Chaotic flavor evolution in an interacting neutrino gas, *Phys. Rev. D* **90**, 025009 (2014).
- [28] A. Mirizzi, G. Mangano, and N. Saviano, Self-induced flavor instabilities of a dense neutrino stream in a two-dimensional model, *Phys. Rev. D* **92**, 021702 (2015).
- [29] B. Dasgupta and A. Mirizzi, Temporal instability enables neutrino flavor conversions deep inside supernovae, *Phys. Rev. D* **92**, 125030 (2015).
- [30] F. Capozzi, B. Dasgupta, and A. Mirizzi, Self-induced temporal instability from a neutrino antenna, *J. Cosmol. Astropart. Phys.* **04** (2016) 043.

- [31] S. Sarikas, D. de Sousa Seixas, and G. G. Raffelt, Spurious instabilities in multi-angle simulations of collective flavor conversion, *Phys. Rev. D* **86**, 125020 (2012).
- [32] G. G. Raffelt, S. Sarikas, and D. de Sousa Seixas, Axial Symmetry Breaking in Self-Induced Flavor Conversion of Supernova Neutrino Fluxes, *Phys. Rev. Lett.* **111**, 091101 (2013); Erratum, *Phys. Rev. Lett.* **113**, 239903(E) (2014).
- [33] G. G. Raffelt and D. de Sousa Seixas, Neutrino flavor pendulum in both mass hierarchies, *Phys. Rev. D* **88**, 045031 (2013).
- [34] G. Mangano, A. Mirizzi, and N. Saviano, Damping the neutrino flavor pendulum by breaking homogeneity, *Phys. Rev. D* **89**, 073017 (2014).
- [35] H. Duan and S. Shalgar, Flavor instabilities in the neutrino line model, *Phys. Lett. B* **747**, 139 (2015).
- [36] S. Chakraborty, R. S. Hansen, I. Izaguirre, and G. Raffelt, Self-induced flavor conversion of supernova neutrinos on small scales, *J. Cosmol. Astropart. Phys.* **01** (2016) 028.
- [37] G. Sigl and G. G. Raffelt, General kinetic description of relativistic mixed neutrinos, *Nucl. Phys.* **B406**, 423 (1993).
- [38] C. Y. Cardall, Liouville equations for neutrino distribution matrices, *Phys. Rev. D* **78**, 085017 (2008).
- [39] S. Abbar and H. Duan, Neutrino flavor instabilities in a time-dependent supernova model, *Phys. Lett. B* **751**, 43 (2015).
- [40] B. Dasgupta, A. Dighe, G. G. Raffelt, and A. Yu. Smirnov, Multiple Spectral Splits of Supernova Neutrinos, *Phys. Rev. Lett.* **103**, 051105 (2009).
- [41] G. Fogli, E. Lisi, A. Marrone, and I. Tamborra, Supernova neutrinos and antineutrinos: Ternary luminosity diagram and spectral split patterns, *J. Cosmol. Astropart. Phys.* **10** (2009) 002.
- [42] A. Mirizzi and P. D. Serpico, Flavor stability analysis of dense supernova neutrinos with flavor-dependent angular distributions, *Phys. Rev. D* **86**, 085010 (2012).
- [43] S. Sarikas, G. G. Raffelt, L. Hüdepohl, and H.-T. Janka, Suppression of Self-Induced Flavor Conversion in the Supernova Accretion Phase, *Phys. Rev. Lett.* **108**, 061101 (2012).
- [44] The neutrino data for the $15 M_{\odot}$ 1D Garching model are available at <http://wwwmpa.mpa-garching.mpg.de/ccsnarchive/index.html>.
- [45] A. Banerjee, A. Dighe, and G. G. Raffelt, Linearized flavor-stability analysis of dense neutrino streams, *Phys. Rev. D* **84**, 053013 (2011).
- [46] B. Dasgupta, G. G. Raffelt, and I. Tamborra, Triggering collective oscillations by three-flavor effects, *Phys. Rev. D* **81**, 073004 (2010).
- [47] A. Esteban-Pretel, R. Tomàs, and J. W. F. Valle, Interplay between collective effects and non-standard neutrino interactions of supernova neutrinos, *Phys. Rev. D* **81**, 063003 (2010).
- [48] A. de Gouvea and S. Shalgar, Effect of transition magnetic moments on collective supernova neutrino oscillations, *J. Cosmol. Astropart. Phys.* **10** (2012) 027.
- [49] I. Tamborra, F. Hanke, H.-T. Janka, B. Müller, G. G. Raffelt, and A. Marek, Self-sustained asymmetry of lepton-number emission: A new phenomenon during the supernova shock-accretion phase in three dimensions, *Astrophys. J.* **792**, 96 (2014).